A modification of the electromigration device and modelling methods for diffusion and sorption studies of radionuclides in intact crystalline rocks

Xiaodong Li[a,*], Shuo Meng[b], Eini Puhakka[a], Jussi Ikonen[a], Longcheng Liu[b], Marja Siitari-Kauppi[a]

[a] Department of Chemistry, University of Helsinki, P.O. Box 55, FI-00014, Finland
[b] Chemical Engineering, Royal Institute of Technology KTH, Stockholm, Sweden

ABSTRACT

To determine the diffusion and sorption properties of radionuclides in intact crystalline rocks, a new electromigration device was built and tested by running with I^- and Se(IV) ions. By introducing a potentiostat to impose a constant voltage over the studied rock sample, the electromigration device can give more stable and accurate experimental results than those from the traditional electromigration devices. In addition, the variation in the pH of the background electrolytes was minimised by adding a small amount of $NaHCO_3$ as buffers. To interpret the experimental results with more confidence, an advection-dispersion model was also developed in this study, which accounts for the most important mechanisms governing ionic transport in the electromigration experiments. Data analysis of the breakthrough curves by the advection-dispersion model, instead of the traditional ideal plug-flow model, suggest that the effective diffusivities of I^- and Se(IV) are $(1.15 \pm 0.06) \times 10^{-13}$ m^2/s and $(3.50 \pm 0.86) \times 10^{-14}$ m^2/s, respectively. The results also show that I^- is more mobile than Se(IV) ions when migrating through the same intact rock sample and that their sorption properties are almost identical.

1. Introduction

The final disposal of spent nuclear fuel is considered to take place in deep geological repositories in many countries (De Cannière et al., 2010; Ewing, 2015; Posiva, 2013). A multiple barrier system, including both engineered and natural, is normally employed to ensure the safety of the disposal. Low-porous crystalline rock, such as granite, is therefore the final natural barrier to provide retardation of radionuclides from migrating into groundwater in most nuclear waste disposal concepts (Muuri, 2015; Posiva, 2012; Söderlund, 2016). The sorption on the pore surfaces of the bedrock and the diffusion into the low-porous rock matrix are the two most significant processes that retard radionuclides migrating through the water conducting fractures of the crystalline rock (Dai et al., 2007; Grisak and Pickens, 1980; Neretnieks, 1980; Posiva, 2013; Séby et al., 1998). For this reason, many studies have been carried out to determine the sorption and diffusion properties of dominant radionuclides existing in nuclear waste, such as Cs^+, Sr^{2+}, I^- and SeO_3^{2-}, by batch sorption experiments (Li et al., 2018; Söderlund et al., 2016a, 2016b), block scale diffusion experiments (García-Gutiérrez et al., 2006; Ikonen et al., 2016b), through-diffusion experiments (Puukko, 2014; Tachi et al., 2015), electromigration experiments (André, 2009; André et al., 2009a; Löfgren and Neretnieks,

2006; Puukko et al., 2018) and He gas through diffusion experiments (Kuva et al., 2015, 2016).

Among these experimental methods, electromigration is getting more attention in the last two decades. This method can provide parameters like effective diffusion coefficient (D_e), distribution coefficient (K_d) and formation factor (F_f) for an intact crystalline rock sample in a much faster way than the traditional through diffusion experiments in water phase, which might take several months (Tachi et al., 2015). Typically, the porosity of the bedrock is in the order of 10^{-3} while the apertures of its micropores are in the order of 10^{-6} m (Möri et al., 2003). As a result, the permeability of the rock matrix is very small and the pore water in the rock matrix could be considered as stagnant. Due to the low porosity and tortuous pores, the diffusion experiments are very time consuming in water saturated rock matrix.

In order to reduce the experimental time by accelerating the transport of charged ions, applications of hydraulic pressure, electric field over the rock sample (electromigration) and gas phase experiments are normally used. Because of the low permeability of the rock sample, extremely high hydraulic pressure is often required to accelerate the movement of tracer ions in rock matrix. Gas phase through diffusion experiments using He atom as a tracer can reduce the experimental time for about 11,000 times (Kuva et al., 2015, 2016).

However, water-based experiments can normally provide more reliable and accurate results because in the gas phase experiments, the chemical effects and other water-phase related interactions (e.g. solute-mineral surface interactions) must be ignored. By contrast, the electromigration method is more advantage because a small electrical field is efficient enough to accelerate the migration of ions in pore water inside a low-permeability granitic rock core (Maes et al., 1999; Mitchell and Soga, 2005). Under the electrical potential gradient, the charged particles and ions can migrate in low porous rock sample about 1000 times faster than elements in water saturated rock, depending on the strength of the electric field. As a result, the experimental time could be reduced significantly to several days.

Another advantage of utilizing electromigration method is that the K_d (equivalently, the retardation factor R) values of intact rock samples could also be determined conveniently. In the batch sorption experiments, which is a traditional way of measuring K_d values, samples are normally crushed which increases significantly the specific surface area of the samples and may give access to otherwise isolated pores. As a consequence, the K_d values determined from crushed rock samples will generally be overestimated (André et al., 2009b; Puukko et al., 2018). To address this problem, conservative estimates of the upscaling factors have been performed prior to use the K_d values in a performance and safety assessment of a geological repository (Puukko et al., 2018). In the electromigration experiments, however, the retardation of sorptive radionuclides for an intact rock sample can directly be evaluated by analysing the mass balance over the rock sample (André et al., 2009a; Puukko et al., 2018).

With this understanding, Löfgren and André designed an electromigration device and tested the migration behaviour of I^- and Cs^+ ions (André, 2009; André et al., 2009a; Löfgren, 2005; Löfgren et al., 2009; Löfgren, 2015; Löfgren and Neretnieks, 2006). The breakthrough time of I^- for example in a 15 mm thick sample was found to be only several hours with an applied potential gradient of 20 V/m or 1000 V/m whereas the effective diffusion coefficients were estimated to be 4.0×10^{-13} m²/s for I^- and 3.0×10^{-13} m²/s for Cs^+, respectively (André et al., 2009a, 2009b). However, some critical flaws still exist in their design of the device as well as in the modelling approaches for analysing experimental results. For example, their device does not include a voltage-self-controlling system, which may cause large experimental errors in long-term studies and even give wrong results. Moreover, the traditional modelling method for analysing results from electromigration experiments involves many unrealistic assumptions and simplifications. The model could only give a rough estimate of the D_e and K_d parameters, which normally contain large uncertainties.

The purpose of this work is to update the electromigration experimental setup and to develop an advection-dispersion model for more accurate analysis of the experimental results. The modified device will have the abilities of voltage-self-controlling, continuous-current-recording and solution-pH-stabilization. Two anions (I^- and SeO_3^{2-}) were studied with the updated electromigration setup under different potential gradients. The advection-dispersion model will, as detailed in our companion paper Meng et al., 2019, account for the most important mechanisms governing ionic transport through an intact rock core, which is subject to an electric field. It enables to give a reliable estimate of the diffusion and sorption properties of the tracer ions in low permeable granitic rock.

2. Materials and methods

2.1. Sample preparation

The rock sample used in the electromigration experiment was collected from Äspö underground laboratory (borehole KLX11F, 17 m depth) in collaboration with Linnaeus University. The length of the rock sample was 1.12 cm, as measured by a caliper, and the diameter was 5 cm. The lithology distribution of the rock sample was quartz monzodiorite (95.5%) and fine-grained granite (4.5%). It was saturated with synthetic groundwater and vacuum packed in a tight vessel before using in the experiment. More detailed information could be found in the report by Mattsson et al. (2007).

The rock samples were dried at 105 °C in a vacuum thermostat oven for at least 4 days to achieve complete dryness. After that, the samples were stored in a desiccator until normal temperature. The dry weights of the samples were, then, measured.

Afterwards, the samples were water saturated with the vacuum method as described by Ohlsson (2000) and Löfgren (2005). First, the samples were placed in a desiccator above 0.2 M NaCl solution. The air in the desiccator was evacuated with a pump and water vapor diffused at low pressure into the sample and saturated the connected micropores of the rock sample. The evacuation process was repeated twice per hour for at least 6 h to get rid of the air leak from the rock sample in the desiccator. Thereafter, the sample was shaken off into the NaCl electrolyte and totally immersed in it. The pressure in the desiccator was, then, increased slowly until atmospheric pressure, in more than 1 day. After achieving atmospheric pressure, the sample was stored in the electrolyte to achieve fully saturation before used in the electromigration experiments.

2.2. Modification of the electromigration experimental setup

2.2.1. Basic design of the electromigration device

As schematically shown in Fig. 1, the electromigration device could be seen as a further implementation of the traditional through-diffusion method. The different is that a constant voltage is applied over the rock sample, which is placed between two chambers, one holding an electrolyte with high concentration tracer (the source chamber) and one holding the same electrolyte initially free of the tracer (the recipient chamber). Since electromigration is the main process of solute transport in this study, only ionic tracers should be considered.

The potential gradients over the rock sample could be achieved by placing an electrode in each of the electrolyte solutions and simply connecting the electrodes to a direct current power supply. In this manner, however, a pH gradient will inevitably evolve within the system, as electrolysis will occur at both anode and cathode:

$$\text{Anode:} 2H_2O - 4e^- \Longleftrightarrow 4H^+ + O_2 \tag{1}$$

$$\text{Cathode:} 2H_2O + 2e^- \Longleftrightarrow 2OH^- + H_2 \tag{2}$$
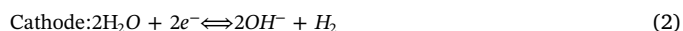
To avoid pH change of the electrolytes caused by electrolysis, Löfgren and Neretnieks (2006), and also André et al. (2009a, 2009b), placed anode and cathode in two end chambers, respectively, that are separated from both the source and recipient chambers, resulting in four chambers in the electromigration setup, as illustrated in Fig. 1. Moreover, by intermixing the anode and cathode electrolytes with two peristatic pumps, the protons and hydroxyl ions that are formed at the electrode surfaces may quickly neutralize with each other. As a result, the pH differences between the anode and cathode electrolytes could significantly be reduced. To avoid short-circuiting in the mixing streams, drop-wise mixing is normally required.

In Fig. 1 the anode and cathode are connected to a direct current power supply through an ampere meter. The potential difference over the rock sample is measured by a voltmeter that is connected to a pair of separate electrodes placed in the source and recipient chambers, respectively.

During the experiment, the tracer ions subjected to an electrical field will be forced to move towards the electrode of opposite charge. As a result of coupling actions of electromigration, electroosmosis and dispersion, the tracer will migrate through the rock sample much faster than if only diffusion would have been the main transport mechanism.

2.2.2. Improvement of the electromigration setup

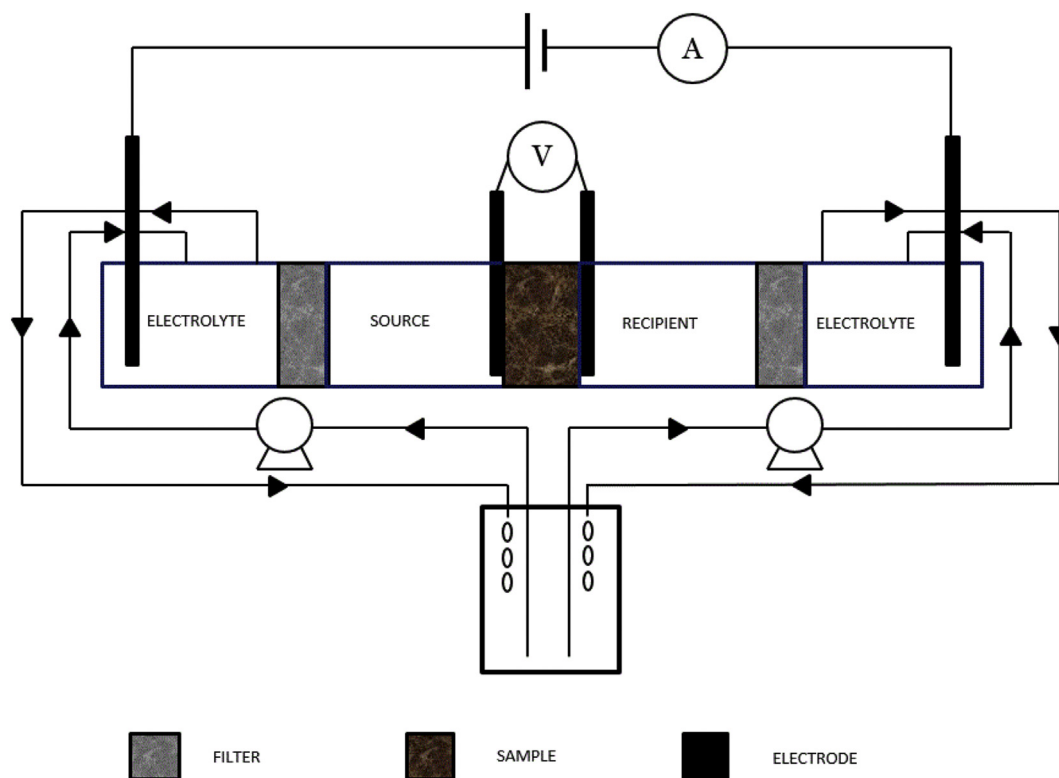The improvement of the electromigration setup was based on the

Fig. 1. Schematic setup for the electromigration experiments (Löfgren and Neretnieks, 2006).

former design of Löfgren and Neretnieks (2006) and also André et al. (2009) described above by considering some points that were not taken into account. The modified device has the functions of voltage-self-controlling, continuous-current-recording and solution-pH-stabilization. It enables to provide more accurate and reproducible results of electromigration experiments. Long term running of the device also becomes possible, because the voltage over the rock sample will be adjusted automatically by the device itself to keep a constant value whenever the resistance of the rock sample changes.

The change in resistance is a result of the concentration evolution of the tracer ions as well as other background ions, such as H^+, OH^- and Na^+ and Cl^-. As suggested by the modelling results with PHREEQC code (Appelo, 2017), the concentration distribution of different ions is changing with the electromigration experiment goes on and it is a function of the distance to the boundary of the rock sample, depending on the diffusion coefficients of the ions.

The change of the concentrations of different ions inside the rock sample is unavoidable during the running of the electromigration device and it leads to the change of the potential difference over the rock sample, if it is not carefully controlled. An inaccurate and variable potential difference over the rock sample will change the transport behaviour of ions in the connective pore network of rock and finally produce large errors in the interpretation of the experimental results. In order to keep a constant voltage over the rock sample, we introduced a potentiostat (CHI 660e made by CH Instruments) into the system to replace the normal power source showed in Fig. 1.

The introduction of a potentiostat brings two important advantages. Firstly, the voltage over the rock sample can be precisely controlled (± 0.01 V) within the experimental period by applying the four-electrode function of the potentiostat (Fig. 2). The four-electrode measuring method is an advanced electrode impedance measuring technique for precise measurement of low resistance values. Separate pairs of electrodes are used in the measurement with four-electrode technique: current carrying electrodes (including Working electrode (W) and Counter electrode (C)) and voltage sensing electrodes (including
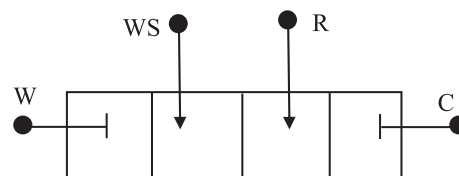

Fig. 2. Schematic illustration of the four-electrode cell setup.

Working Sense electrode (WS) and Reference electrode (R)). More accurate results than the normally used two electrode setup will be achieved by applying four-electrode technique. With this improvement, the voltage difference over the rock sample can be sensed and kept constant by WS and R electrodes and the current going through the whole device can be supplied by W and the C electrodes. The whole voltage over the electromigration device and the current going through the device can, therefore, be adjusted by the potentiostat according to the change of the resistance of the pore solution, to guarantee a constant potential gradient over the rock sample. In this manner, the stability of the device can be improved significantly.

Secondly, the current flowing through the rock sample can be recorded automatically and continuously. Since variation in the current gives information of the movement and distribution of ions inside the rock sample under an electrical field, it is an important factor to be considered when analysing the experimental results. The current change has not been recorded or modelled carefully in previous studies during the electromigration experiments.

Though the electromigration device was designed to separate the electrode chambers and tracer chambers to reduce the influence of pH change on aqueous chemistry, pH would still slightly change during the electromigration experiments. One reason for this is that the migration of H^+ and OH^-, which generate at the electrodes as a result of electrolysis (Eqs. (1) and (2)), are much faster than the migration of other ions in the background solutions like Na^+, Cl^- and the studied tracer ions. According to the phreeqc.bat database file of PHREEQC computer

program (Appelo and Postma, 2004), H^+ diffuses 7 times faster than Na^+, and about twice faster than OH^-. This means that much more amount of H^+ and OH^- would migrate into the tracer chambers than the amounts of other ions into the recipient chamber. In addition, the dissolution or precipitation of the minerals in the rock matrix would also cause the pH change of the background electrolytes.

The evolution of the pH gradient over the rock sample could cause a number of problems in the electromigration experiments. Some ionic tracers, for example SeO_3^{2-}, may become protonated ($HSeO_3^-$) and deprotonated if the pH changes. This will change the overall charge of the Se(IV) ions. Under strong acidic or basic pH conditions the precipitation and dissolution of minerals will become severe and this may affect the transport properties of the rock sample. In addition, the efficiency of transferring current from the electrodes to electrolytes decreases if pH changes are allowed in the electrolytes.

To stabilize pH values of the background electrolytes during the running of electromigration experiments, we buffered the solution by replacing the NaCl solution, which was commonly used as background electrolyte in previous studies, by 0.2 M NaCl and 0.002 M NaHCO₃ solutions, the pH values of which were adjusted to be ~8.5 before using. The addition of NaHCO₃ has two functions. Firstly, NaHCO₃ simulates the pH level of real groundwater while the concentration of NaCl simulates the ionic strength. Secondly, $HCO_3^- \sim CO_3^{2-}$ in the solution is a pH-buffer pair. Even if some amount of H^+ or OH^- migrate into the tracer chambers from the electrode chamber, they would not cause significant changes in the pH value because of the buffer effect of $HCO_3^- \sim CO_3^{2-}$ pair.

2.3. Electromigration experiments

2.3.1. Porosity measurement

The porosity of the rock sample was measured by a water gravimetry method (Melnyk and Skeet, 1986; Ohlsson, 2000). After achieving fully saturation in a specific NaCl electrolyte, the weight of the rock sample as a function time was recorded continuously during the drying process. This allows us to determine the surface dry weight of the rock sample from the intersection between two lines on the time-based drying curve. The intersection point was interpreted as the weight of sample with totally dry surface when evaporation of the pore water has been ceased (see Section 3.1, Fig. 4)

The volume of the rock sample was determined by immersing it into 0.2 M NaCl electrolyte and measuring the weight difference before and after the immersing procedure. The density of the electrolyte was determined by measuring the weight of a specific volume of the liquid.

The volume of the pores in the rock sample can, thus, be calculated by the weight difference between the saturated and dried rock sample together with the density of the electrolyte. The ratio of the pore volume to the rock sample volume gives the porosity of the rock sample.

2.3.2. Electromigration setup

As shown in Fig. 3, the new electromigration setup was built in accordance with the modification ideas discussed in Section 2.1. The material used for the updated electromigration device is poly (methyl methacrylate) PMMA, which is both transparent and hard. This material facilitates the observation of the running conditions inside the cells and it is hard enough to ensure tightness. The volume of the source and recipient chambers is 152 ml while the volume of the two electrode chambers at both ends is 250 ml. The four electrode plates with a dimension of 1 cm × 2 cm is made of titanium metal. A copper string was used to connect the titanium electrodes, and voltage and ampere meters were used to observe the instant voltage over the rock sample and the current going through the whole device, respectively.

The Amperometric i-t curve technique (i-t) of the potentiostat was used to control the four-electrode system. A constant potential of 2 V or 4 V was applied over the rock sample and the current going through the device was recorded continuously as a function of experimental time.

The sample was fitted in a PMMA cylindrical shell which has the same inner diameter as the diameter of the rock sample. Before inserting the sample inside the cylindrical shell, both the outer surface of the sample and the inner surface of the cylindrical shell were glued with epoxy (Loctite, dry in 5 min, full strength in 24 h) to tightly glue them together. The purpose is to make sure that all the tracer ions can only migrate through the rock sample by its micropores. Then, the sample holder was left in the open air for 30 h before it was placed in the electromigration device to guarantee total strength of the epoxy.

The other two rock samples with the length of 1 cm were used as filters to separate the electrolyte in the two electrode chambers from the electrolyte in the tracer chambers. The mineralogical compositions of the two filters were similar with the rock sample tested in electromigration experiments. The holders for the two filters were made in the same way as that for the sample holder.

2.3.3. Electromigration measurements

Three tracers were tested separately with the electromigration device; quinoxaline (Sigma-Aldrich, 99%) for electroosmosis measurements, Na₂SeO₃ for Se(IV) diffusion tests and NaI for I^- diffusion tests. Iodide is known to be a non-sorbing ion on mineral surfaces (Ikonen et al., 2016a) while the Se(IV) ions (SeO_3^{2-} or $HSeO_3^-$) are believed to be slightly sorbing on mineral surfaces under the low saline groundwater conditions (Ikonen et al., 2016b; Li et al., 2018). The background electrolyte was 0.2 M NaCl and buffered by 0.002 M NaHCO₃ as shown in Section 2.2.

The voltage over the rock sample was set to be 2 V or 4 V, and was kept constant by the potentiostat. Before running the electromigration experiments with tracers, the device was stabilized by running it with background electrolyte under the applied voltage for 3 days to saturate the rock sample with background electrolyte. The stabilization of the device can be observed by the recorded current data when a stable state is seemingly reached. After stabilization, tracers (quinoxaline or Na₂SeO₃ or NaI chemicals) were added into the source chamber, resulting in the final concentration of the tracers being 0.1 M. To balance the ionic strength throughout the through-electromigration cell, NaCl with the same ionic strength as the tracer was immediately added into the recipient chamber. The initial conditions of the electromigration experiments are summarized in Table 1.

After addition of the tracers, the source and recipient chambers were both stirred for 5 min by magnetic stirrers. At the same time, two samples of 2 ml were taken from the chambers to determine the original concentration of the tracer ions in the beginning of the experiment. After sampling, the same amount of background electrolyte was added into the chambers to keep the hydraulic pressure and the volume of solutions to be constant.

During the experiments, the source and recipient chambers were stirred by magnetic stirrers all the time at a speed of 250 rpm. The concentrations of tracers in the recipient chamber were followed by sampling and adding the same amount of background electrolyte.

The concentrations of quinoxaline were measured by a UV–VIS spectrophotometer (Thermo Scientific, Genesys 10s UV–Vis). According to the spectrum (NIST Chemistry WebBook, SRD 69, 2018), the highest peak of quinoxaline spectrum appears at ~270 nm and this peak was used to analyse the concentration of quinoxaline.

The concentrations of Se and I were analysed by ICP-MS (Agilent 7800). All the samples were stored in acid-washed tubes. After dilution and filtration, Se samples were acidified by adding strong suprapure HNO₃ (Romil) until 0.5 M and the concentration of Se was analysed by isotope [82]Se. Because of high volatility of iodine at low pH conditions, 5% tetramethylammonium hydroxide (TMAH) was used as background electrolyte for I concentration measurements by ICP-MS. The concentration of I^- was analysed by detecting the concentration of isotope [127]I. The detection limit of 0.006 μg/g in pure solution was validated using helium as a reaction gas in the reaction chamber (Ikonen, 2017; Ikonen et al., 2016a).
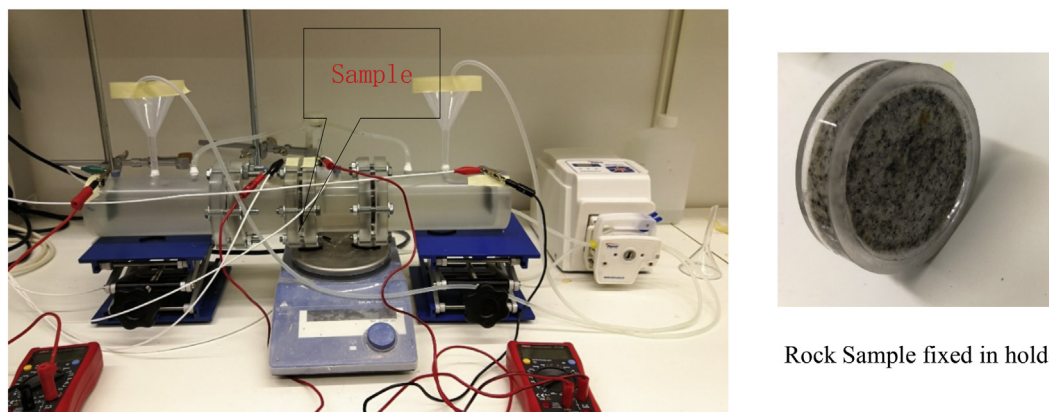
Rock Sample fixed in holder

Fig. 3. Left: setup of the electromigration experiments. The sample is in the middle of the setup between the source chamber and the recipient chamber. At both ends are the two electrode chambers separated by two rock filters from the tracer chambers. Right: Sample/filter holder designed for the electromigration setup.

2.4. Update of data analysis approach

By following the concentration change of the tracer ions in the recipient chamber, a breakthrough curve, which is used to estimate the diffusion and sorption properties of the tracer ions, can be obtained from the experiment. To interpret the breakthrough curve data, a model that can account for the most important mechanisms governing ionic transport in the electromigration experiments is required. In the following section, the traditional ideal plug-flow model and newly developed advection-dispersion model are shortly presented.

2.4.1. Ideal plug-flow model

Due to the simplicity of its use, the ideal plug-flow model has been recently applied to interpret the experimental results of electromigration (André et al., 2009). It accounts only for the effect of electromigration, the most important mechanism on ionic transport in electrical field. The contributions of electroosmosis and dispersion are, however, entirely omitted (Meng et al., 2019). As a result, one only needs to make a linear regression of the late-time breakthrough curve, over which the tracer concentration increases seemingly in a constant rate (André et al., 2009). The intercept of the regression line with the time coordinate gives an estimate of the apparent advection time, whereas the slope of the regression line approximates the rate of change of the tracer concentration in the recipient chamber, from which the effective convection velocity or the effective mass flux can be estimated.

The use of the law of Einstein (Atkins and Paula, 2009) for the relation between diffusivity and ionic mobility allows the effective diffusion coefficient (D_e) to be estimated from the slope (dc/dt) of the regression line by (André et al., 2009),

$$D_e = \frac{V \bullet k \bullet T \bullet \frac{dc}{dt}}{A \bullet c_t \bullet e \bullet z \bullet \frac{d\phi}{dx}} \tag{3}$$

where V (m^3) is the volume of the recipient chamber, k (m$^2 \cdot$kg$\cdot$s$^{-2} \cdot$K^{-1}) is the Boltzmann constant, A (m^2) is the cross section area of the rock sample, c_t (mol/m$_3$) is the test concentration in the supply chamber, e (C) is the electron charge and $d\Phi/dx$ (V/m) is the electrical potential

gradient applied to the rock sample.

Moreover, the ideal plug-flow model used by André et al. (2009) implicitly assumes that the tracer flux into the rock sample is constant during the experiment and that the rock sample has been fully in equilibrium with the tracer concentration in the source chamber after the breakthrough time. This is not the real case but it facilitates evaluation of the K_d value of the test tracer by making a mass balance of the tracer ions over the rock sample, giving:

$$K_d = \frac{V \bullet \frac{dc}{dt} \bullet t_{br} - V_r \bullet \varepsilon_t \bullet c_t}{m \bullet c_t} \tag{4}$$

where t_{br} (s) is the breakthrough time determined by the intercept of the linear regression line with the time axis of the breakthrough curve, V_r (m^3) is the volume of the rock sample, c_t (mol/m^3) is the source concentration of the tracer ions in the supply chamber and m (kg) is the mass of the sample.

It follows that the retardation factor, defined as

$$R = 1 + \frac{\rho K_d}{\varepsilon_{TS}} \tag{5}$$

can also be determined, where ρ is the dry bulk density of the rock sample, and ε_{TS} is the connective porosity available for the tracer ions.

It should, however, be noted that the above three expressions are valid only under the assumption that the tracer concentration in the source chamber (c_t) remains constant during the running of the experiments. Since, in practice, only $1/10^5$ or $1/10^6$ fraction of the tracer ions may migrate through the rock sample within the limited experimental time, we can reasonably ignore the change of the source concentration so as to simply apply Eqs. (3)–(5) for data analysis.

2.4.2. Advection-dispersion model

To interpret the experimental results more accurately with great confidence, we developed an advection-dispersion model that well simulates the important processes in the through-electromigration experiment. It accounts for not only the dominant effect of electromigration but also the contributions of electroosmosis and dispersion on ionic transport. As detailed in our companion paper (Meng et al., 2019), the advection-dispersion model was formulated on the basis of

Table 1
The initial conditions of the electromigration experiments. The tracers were tested separately with the electromigration device.

Tracers	Conc. in source chamber (M)	Conc. in recipient chamber (M)	Voltage over the rock sample	Background electrolytes[a]
Quinoxaline	0.1	0	2 V and 4 V	0.2 M NaCl + 2 mM NaHCO$_3$
NaI	0.1	0	2 V and 4 V	0.2 M NaCl + 2 mM NaHCO$_3$
Na$_2$SeO$_3$	0.1	0	2 V and 4 V	0.2 M NaCl + 2 mM NaHCO$_3$

[a] The pH of the background electrolytes was adjusted to be 8.5 by adding NaOH before adding to the electromigration device.

the equation of continuity describing the mass balance of the tracer ions over a rock sample perpendicular to the direction of mass transport, i.e.,

$$\varepsilon_{TS} R \frac{\partial c}{\partial t} = -v_c^e \frac{\partial c}{\partial x} + D^e \frac{\partial^2 c}{\partial x^2} \tag{6}$$

where v_c^e is the effective convection velocity compose of the contributions of both electromigration and electroosmosis, and D^e is the effective dispersion coefficient, which can be approximated by (Beauwens et al., 2005),

$$D^e = \alpha v_c^e + D_e \tag{7}$$

where α is the dispersion length.

For the electromigration experiments under consideration, the full solution of the advection-dispersion model can be written in the Laplace domain as:

$$\overline{c_R} = -\frac{\exp\left(\frac{Pe}{2}\right)\frac{Scsch(S)}{Pe}}{\left[\frac{1}{2} + \beta_L s + \frac{Scoth(S)}{Pe}\right]\left[\frac{1}{2} - \beta_R s - \frac{Scoth(S)}{Pe}\right] + \left[\frac{Scsch(S)}{Pe}\right]^2}\beta_L c_0 \tag{8}$$

with

$$Pe = \frac{v_c^e l}{D^e} \tag{9}$$

and

$$S = \frac{Pe}{2}\sqrt{1 + \frac{4\tau_A s}{Pe}} \tag{10}$$

where s is the Laplace variable, and τ_A is a characteristic advection time, i.e.,

$$\tau_A = \frac{\varepsilon_{TS} RL}{v_c^e} \tag{11}$$

The inverse Laplace transform of Eq. (8) would, then, give the tracer concentration c_R at the recipient chamber and it can, for a given experimental setup, be generally written as,

$$c_R = f(v_c^e, D_e, \varepsilon_{TS} R, c_0, t) \tag{12}$$

This result indicates that the numerical solution of c_R, obtained by use of e.g. De Hoog algorithm (de Hoog et al., 1982) to numerically transform Eq. (8) back to the time domain, would depend only on v_c^e, D_e and $\varepsilon_{TS} R$. As a consequence, these parameters can readily be evaluated by fitting the numerical solution c_R to the measured data of the breakthrough curve using e.g. a nonlinear least squares algorithm (Meng et al., 2019), supplemented with suitable lower and upper bounds.

3. Results

3.1. Porosity

The drying curve, obtained as described in Section 2.2, is shown in Fig. 4. The two linear lines represent the evaporation of water from the sample surface and the evaporation of water from the pore space, respectively. The interaction of the two lines indicates the weight of rock sample with totally dry surface while fully saturated pore space. With the data presented in Fig. 4, we estimated that the porosity of the rock sample used in our experiments is 0.7% ± 0.4%.

The assumption here is that the connected porosity of the cm-scale rock sample is determined by water gravimetry. The total porosity which here means the connected porosity is equal to the diffusion porosity in the sample type used in this work. The sample is fine to medium grained granitic rock without cm-scale micro fractures in it The porosity including flow, diffusion and residual parts is defined by Norton and Knapp (1977). Here we do not have the flow porosity and the residual porosity is not taken into account since it can not be revealed by water gravimetry method. Thus, we assume that the water
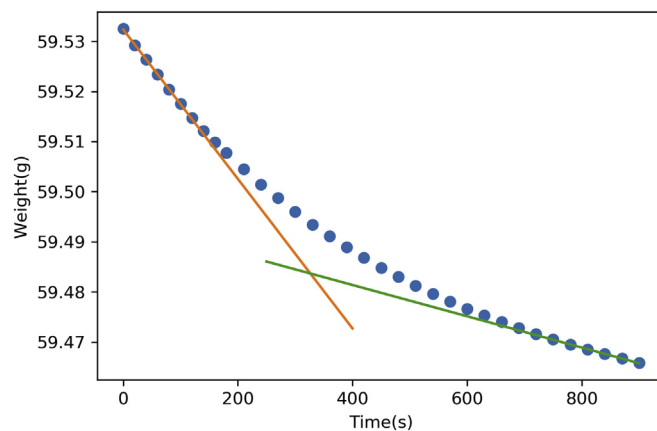

Fig. 4. The drying curve of the rock sample used in the electromigration experiment. The two lines represent the processes of out-surface dryness and the evaporation of the pore water, respectively.

gravimetry result of porosity (0.7 ± 0.4%) is fully usable in the diffusion process and the result will be used in the following modelling exercises. However, we also agree that more sophisticated modelling approaches need more detailed porosity data, such as pore apertures, tortuosity and constrictivity, mineral specific porosity and heterogeneities of porosity patterns in cm-scale.

3.2. Electroosmosis

The influence of electroosmosis on ionic transport was determined by running quinoxaline through the electromigration device. The measurement was performed for several times, before the running of Se and I tracers; each experiment took 3–5 days. The results did not show obvious detection of quinoxaline in the recipient chamber, even after 5 days measurements. The highest observation was that electroosmosis might account for 4.1% of the total electromigration process. It was, therefore, deemed that the effect of electroosmosis was not a determining factor for the electromigration results and it can be omitted when dealing with data analysis.

3.3. Electromigration with NaI

Two voltages (2 V or 4 V) over the rock sample were applied in the electromigration experiments of NaI using the updated device. The potential gradients over the rock sample were 179 V/m and 357 V/m, respectively. The original concentration of NaI in the source chamber was 0.1 M and the concentration of I^- in the recipient chamber was followed for about 2 days. The breakthrough curves as a function of experimental time recorded by potentiostat are shown in Fig. 5.

The two analysis approaches described in Section 3 (ideal plug-flow model and advection-dispersion model) were applied for analysis of the experimental results. First, the traditional ideal plug-flow model was tried by drawing a linear regression line with the last several data points where a pseudo steady state seemed to be established. The breakthrough time for I^- migrating through the rock sample and the concentration change rate of the I^- ions in the recipient chamber can be evaluated from the intercept and the slope of the linear regression line, as given in Table 2.

The numerical solution of the advection-dispersion model in Laplace domain (Eq. (8)) can be easily achieved by D_e Hoog algorithm (de Hoog et al., 1982). The results show that the evolution of the tracer concentration in the recipient chamber would depend on v_c^e, D_e and $\varepsilon_{TS} R$ (Eq. (12)). These parameters could simultaneously be evaluated by fitting the numerical solution C_R to the measured data of the breakthrough curve. The D_e values deduced from the advection-dispersion model are listed in Table 2 as D_e^*. The methodology for detailed
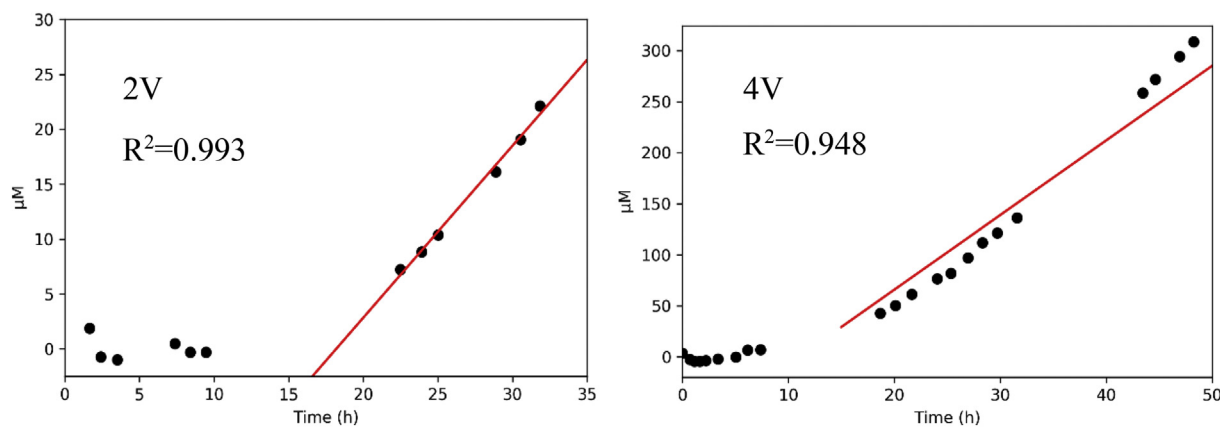
Fig. 5. The concentration of I^- (μM) followed in the recipient chamber as a function of time with 0.1 M NaI in the source chamber. The voltage over the rock sample was 2 V and 4 V, respectively.

analysis of the experimental results can be found in the companion paper (Meng et al., 2019).

According to earlier data reported by Skagius and Neretnieks (Skagius, 1986; Skagius and Neretnieks, 1983), the effective diffusion coefficient of I^- in granites and gneisses is in the range of 1×10^{-14} m²/s to 7×10^{-13} m²/s. The calculated D_e data, both from the traditional method with Eq. (3) and the newly developed advection-dispersion model, are in good agreement with the data reported in literature. Compared with the electromigration data reported in André et al. (2009) work in which only 1.5 h was needed to break through a 15 mm length rock sample under the potential gradient of 200 V/m, the breakthrough time obtained in our experiment was much longer. André et al. (2009) used 0.01 M NaI as the tracer and 0.99 M KCl as the background electrolyte and the D_e of I^- obtained using ideal plug-flow model was 4.0×10^{-13} m²/s, which is 5 times larger than the value estimated from our work. The inconsistence between these experimental results may come from the different physical properties of the rock sample. André et al. (2009) did not show the porosities and the compositions of the rock sample used in their work, however the properties of the rock sample are expected to have a significant effect on the experimental results.

3.4. Electromigration with Na₂SeO₃

The same rock sample used for the electromigration tests of NaI was also tested for Na₂SeO₃ as a tracer under the same experimental conditions. The original concentration of Na₂SeO₃ in the source chamber was also 0.1 M. The same voltage as in the NaI tests, either 2 V or 4 V, was applied over the rock sample. In the recipient chamber, the concentration of Se was followed for about 2 days. The breakthrough curves as a function of experimental time recorded by the potentiostat are shown in Fig. 6.

The breakthrough time and the slope data deduced from the linear regression line as well as the D_e values calculated from Eq. (3) and the advection-dispersion model are given in Table 3. The D_e values calculated by both methods are in the magnitude of 10^{-14} m²/s, in consistent with the recommended values of Se in granite (Ohlsson and Neretniks, 1997).

More importantly, we observed in Figs. 6 and 7 that for both tracer

ions, a clear breakthrough time can be identified from the measured breakthrough curve itself. Before the breakthrough time, the concentration of tracer ions in the recipient chamber remained apparently at the background level. This indicates that the electromigration device was in a good condition of tightness and thus all the tracer ions have migrated through the rock sample by the connective pore network. In addition, comparison of the experimental results also showed a larger breakthrough time and a smaller increase in the rate of the concentration change in the recipient chamber when 2 V was applied over the rock sample instead of 4 V, in both I and Se(IV) experiments. As a conclusion it can be stated that the updated device of electromigration worked well, and that the experimental results can be used confidently to determine the diffusion and sorption properties of the tracer ions.

However, it is noted especially in Fig. 7 that the measured breakthrough curve shows a clear curvature at the moment around the breakthrough time, which is certainly overestimated by the ideal plug-flow model. This signifies actually that dispersion has played a non-negligible role in the ionic transport through the rock sample. As a consequence, application of the ideal plug-flow model for parameter identification can be problematic because it ignores the effect of dispersion and uses only a small portion of the late-time experimental results. In some cases, the selection of the experimental data for linear regression itself also causes trouble because no clear rule can be followed.

3.5. Current data

Fig. 7 shows one of the examples of current evolution during the electromigration experiments. It is obvious that the current going through the rock sample was changing all the time. This is caused by the variation of the ion distribution inside the rock sample, so that the resistances of the rock sample and the two filters are varying all the time. Without a potential controlling system, the inconstant voltage over the rock sample would make the experimental results difficult to interpret.

The current data provided by the potentiostat is also valuable when we try to analyse the ion distribution and diffusion behaviour inside the rock sample. The interpretation of the current data requires consideration of the electric flux of the ions, the chemical and electrical

Table 2

Electromigration results of 1.12 cm rock sample using 0.1 M NaI as tracer and 4 V and 2 V voltages over the rock sample.

Voltage (V)	Length (cm)	Voltage gradient (V/m)	Breakthrough time (h)	Slope (μM/h)	Retardation factor R (−)	D_e (m²/s)	D_e^* (m²/s)
2	1.12	179	18.2	1.57	1	$8.33 \pm 3.25 \times 10^{-14}$	$1.15 \pm 0.06 \times 10^{-13}$
4		357	11.0	7.31	1		

D_e^*: The effective diffusion coefficient of NaI tracer evaluated from the advection-dispersion model.
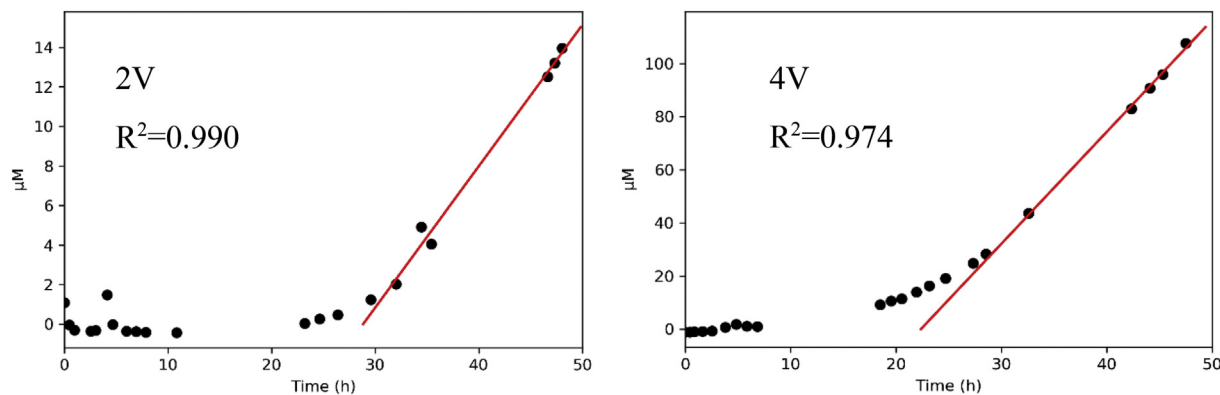
Fig. 6. The concentration of Se (μM) followed in the recipient chamber as a function of measurement time in the electromigration experiments with 0.1 M Na$_2$SeO$_3$ in the source chamber. The voltage over the rock sample was 2 V and 4 V, respectively.

reactions, the individual movement of the ionic species etc., which means that a reactive transport model should be developed for the interpretation of the results. It should take into account not only the effects of electromigration, electroosmosis, and dispersion, but also the effects of aqueous chemistry, i.e. the interactions between the tracer ions and the background electrolytes and the mineral surfaces. Only by this reactive transport model, could the current data shown in Fig. 7 be properly interpreted. In our companion paper (Meng et al., 2019), a reactive transport model was preliminarily developed using the PHREEQC module of electromigration.

4. Discussions

One of the key problems of performing electromigration experiments is the controlling of the voltage over the rock sample. In this work, we introduced a potentiostat to solve the problem. By using the four-electrode function of the potentiostat, the voltage over the rock sample can be adjusted automatically and controlled constantly (± 0.01 V) at the set value. As a result, the experimental errors were significantly reduced in our work. Compared with the electromigration results reported in literature (André et al., 2009a; Löfgren et al., 2009; Löfgren and Neretnieks, 2006), the breakthrough curves as well as the D$_e$ values obtained from the new designed electromigration device are more stable.

Since our main purpose is to estimate the diffusion and sorption properties of the tracers in low porous intact granitic rock, it is preferable first to develop an advection-dispersion model, that account for the most important mechanisms governing ionic transport but ignores the effect of aqueous chemistry. The advection-dispersion model developed in this work avoids the use of many unrealistic assumptions associated with the ideal plug-flow model and succeeds to give reliable results with small uncertainties. The ideal plug-flow model should only be used to define the lower and upper bounds of the corresponding parameters like D$_e$ values. For more accurate analyses of the experimental results, the advection-dispersion model is recommended. One example showing the difference of the two models is given in Fig. 8. The ideal plug-flow model simply makes a linear regression of the data at which a steady state seems to be achieved after the breakthrough time. The intercept of the regression line with the time axis gives an estimate of the advection time, which was assumed to be the breakthrough time;
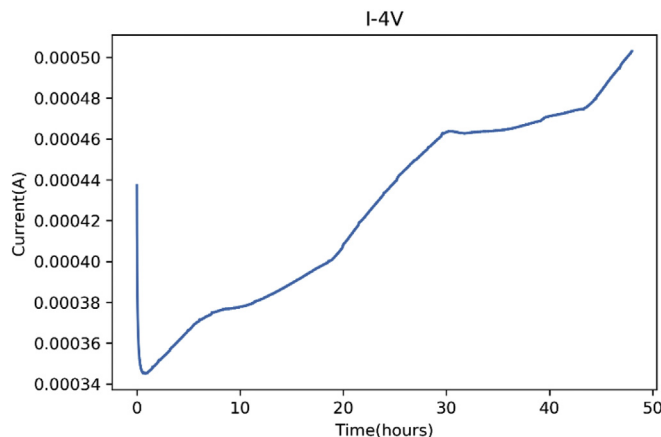

Fig. 7. The current (A) evolution during the electromigration experiments of NaI with 4 V voltage over the rock sample.
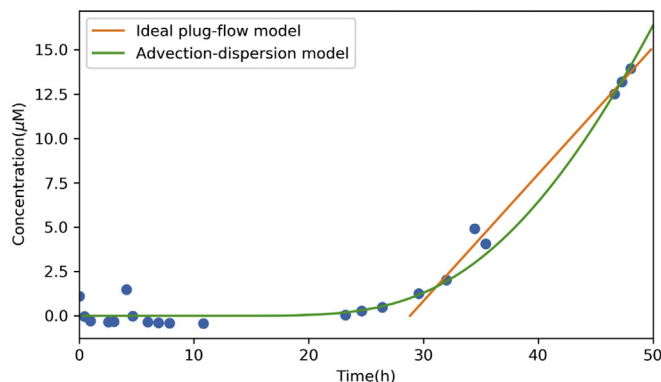

Fig. 8. Comparison of the results of the traditional ideal plug-flow model and the advection-dispersion model for the case of electromigration experiments with 0.1 M Na$_2$SeO$_3$ background solution and 2 V voltage difference over the rock sample.

Table 3

Electromigration experimental results of 0.1 M Na$_2$SeO$_3$ with voltages 4 V and 2 V voltage over 1.12 cm length rock sample.

Voltage (V)	Length (cm)	Voltage gradient (V/m)	Breakthrough time (h)	Slope (μM/h)	Retardation factor R (−)	D$_e$ (m^2/s)	D$_e$* (m^2/s)
2	1.12	179	28.8	0.72	1	$2.30 \pm 0.89 \times 10^{-14}$	$3.50 \pm 0.86 \times 10^{-14}$
4		357	22.4	4.21	1		

D$_e$*: The effective diffusion coefficient of NaI tracer evaluated from the advection-dispersion model.
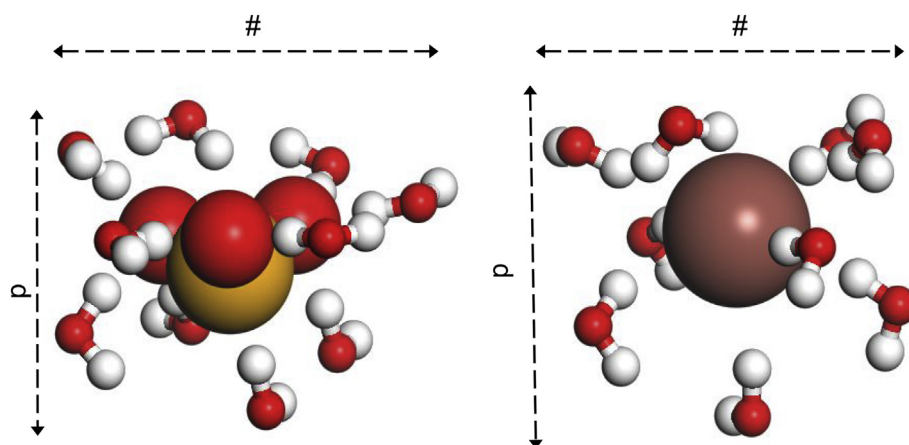
Fig. 9. Schematic representation of the hydration distances found in the SeO_3^{2-} (left) and I^- (right) ions modelled by CASTEP code implemented into Materials Studio.

the slope of the regression line gives an estimate of the rate of the concentration change in the recipient chamber. This method gives a quick but rough estimate of the parameters with large uncertainties. The advection-dispersion model analyses the whole breakthrough curve instead, and more factors that could affect the results can be taken into account by fitting the breakthrough curve obtained from the electromigration experiments with a non-linear least square algorithm.

In the batch sorption experiments, Se(IV) ions are considered to be slightly sorbing onto mineral surfaces. The batch sorption experiments performed by Li et al. (2018) gave the K_d values of Se(IV) sorption onto crushed Grimsel granodiorite being in the range of $(1.7–4.0) \times 10^{-3}$ m^3/kg when Se(IV) concentration ranged from 10^{-6} mol/L to 10^{-3} mol/L in low saline groundwater simulant. However, our analysis of advection-dispersion modelling showed that both I^- and Se(IV) ions are effectively non-sorbing in the intact rock sample investigated in the experimental conditions. The retardation factor calculated from the models are always equal to one and the assumption of I^- and Se(IV) as sorbing species will make the curvature of the simulated breakthrough curves deviate clearly from the obtained experimental data. This result is reasonable considering that the K_d values reported by Li et al. (2018) were obtained from batch sorption experiments with crushed minerals. The crushing process of the mineral will significantly increase the specific surface area of the mineral sample and give an access to the isolated pore and new surfaces inside the minerals. If the K_d values from the work of Li et al. (2018) are corrected with specific surface area, as they pointed out in their work already, the K_d values would be in the range of $(1.3–3.2) \times 10^{-5}$ m^3/kg. Since the values are very small, selenite can be regarded as a slightly sorbing ion on intact rock samples. However, considering the nuclear waste repository that is hundreds of square meters scale and the existence of high sorptive clay minerals at the fracture surfaces in bedrock, the retardation of the Se or I still can not be neglected in the whole concept.

One of the advantages of electromigration experiments, compared with traditional batch sorption experiments, is that K_d values of intact rock samples can be deduced and used directly in the safety assessment of a nuclear waste repository. To use the K_d values from batch sorption experiments, an upscaling factor must be developed to convert the results of batch sorption experiments to use the batch K_d values for the safety assessments of a nuclear waste repository. In practice, it has been shown that the variations of the upscaling factors are rather high which reduces the applicability of the upscaling method (Puukko et al., 2018). In future more work should be done for the sorption studies with electromigration method, taking into account factors like composition of the rock sample, properties of the tracer ions and the salinity of the background electrolyte. The main composition of the rock sample used

in this work is quartz monzodiorite, as we presented in Section 2.1. On the site where the sample was taken, the most dominant minerals in the sealed and open fractures are calcite, chlorite and quartz. The minerals that can sorb selenium effectively, such as kaolinite and biotite are not present. More sorption may be observed if sorptive minerals are present in the composition of the studied rock samples.

The diffusion of I^-, compared to that of Se(IV) ions, is 2 or 3 times faster in the intact rock sample investigated. This result is in consistent with the diffusion coefficients of them in aqueous solutions. In the condition of infinite dilution, the diffusion coefficient of I^- is 2.048×10^{-9} m^2/s while that of selenate is 1.008×10^{-9} m^2/s (CRC Press, 2018). The slow diffusion of Se(IV) ions is attributed to its unsymmetrical dimensions and larger interaction with water molecules. In aqueous solutions, the effective hydrated radius of I^- was reported to be ~ 0.331 nm (Yu and Neretnieks, 1997), while the geometrical structure of SeO_3^{2-} is more complicated since it is an oxoseleno anion. The study of Eklund (2014) by LAXS measurements suggested that the Se–O bond distance in the hydrated ion is 1.709 Å. The $O_w \cdots O_w$ distance in bulk water is 2873 Å, outside of the bound oxygens the proximal $Se \cdots O_w$ distance is 3,87 Å. For distal $Se \cdots O_w$ outside of the lone electron-pair the distance is 4.36 Å. Based on these data, the schematic figure of hydrated SeO_3^{2-} and I^- ions calculated by molecular modelling in water media is shown in Fig. 9. The calculation was performed by evaluating the optimized structures of $SeO_3^{2-} \cdot (H_2O)_{10}$ and $I^- \cdot (H_2O)_9$ ions using CASTEP, i.e. CAmbridge Serial Total Energy Package (Clark et al., 2009) code implemented into BIOVIA Materials Studio 2017 R2. It was based on solving the total electronic energy and overall electronic density distribution in order to define the energetically stable structures for ions (Leach, 2001). According to the molecular modelling results, SeO_3^{2-} are slightly larger and unsymmetrical than I^-, which would cause delay in diffusion when it migrates through the micropores of the intact rock samples.

5. Conclusions

In this work, a new electromigration device was developed and tested by running with I^- and Se(IV) ions. It was found that the new electromigration device can give stable and convincing experimental results, due mainly to the introduction of a potentiostat which could keep the voltage over the rock sample nearly constant during the experiments by adjusting the overall voltage applied to the whole device. At the same time, the pH of the background solutions was also stabilized by adding $NaHCO_3$ buffer. These modifications improve the stability of the experimental conditions and reduce the experimental errors significantly.

To facilitate interpretation of the experimental results, an

advection-dispersion model was developed in this work. It accounts for not only the dominant effect of electromigration but also the contributions of electroosmosis and dispersion on ionic transport, and therefore it can provide better parameter identification with smaller uncertainties than the traditional, ideal plug-flow model, which involves many unrealistic assumptions.

By interpreting the breakthrough curves with both ideal plug-flow model and the advection-dispersion model, the experimental results with quinoxaline as tracer showed that the effect of the electroosmosis can be omitted. The D_e values deduced for I^- diffusion were $(8.33 \pm 3.25) \times 10^{-14}$ m^2/s from ideal plug-flow model and $(1.15 \pm 0.60) \times 10^{-13}$ m^2/s from advection-dispersion model, respectively. The D_e values for Se(IV) ions diffusion were $(3.49 \pm 2.76) \times 10^{-14}$ m^2/s from ideal plug-flow model and $(3.50 \pm 0.86) \times 10^{-14}$ m^2/s from advection-dispersion model, respectively. Furthermore, our analysis suggested that both I^- and Se(IV) ions should be considered as non-sorbing ions when transporting through the studied intact rock sample. The reason why Se(IV) ions migrate relatively slow in comparison with I^- is attributed mainly to its smaller effective diffusion coefficient resulting from its larger and unsymmetrical dimensions.

The new electromigration device and the advection-dispersion model developed enable rapid estimation of the D_e and K_d values from experimental results of the intact rock sample. However, further studies should be applied to justify this method as an appropriate technique for studying diffusion of radionuclides under nuclear waste repository conditions. Here only two sets of experimental results with applied voltages of 2 V and 4 V were available for both I^- and Se(IV) ions by the updated device. Further improvements could be done by applying 5 or more voltages applied over the rock sample to decrease the uncertainties associated with parameter evaluation of the experimental results. Information about the connected pore network and rock mineralogy should also be determined using methods like X-ray tomography, C-14-PMMA autoradiography and electron microscopy to reveal the realistic pore network in the studied rock samples. The combination of these techniques can be used to improve the interpretation of the electromigration data.

Declaration of competing interest

The authors declare that they have no known competing financial interests or personal relationships that could have appeared to influence the work reported in this paper.

Acknowledgements

Authors' statement

Xiaodong Li: Conceptualization, Methodology, Software, Validation, Investigation, Data Curation, Writing-Original Draft, Writing-Review & Editing, Visualization.

Shuo Meng: Conceptualization, Methodology, Software, Formal analysis, Data Curation.

Eini Puhakka: Methodology, Software.

Jussi Ikonen: Methododlgy.

Longcheng Liu: Methodology, Software, Formal analysis, Resources, Supervision, Project administration, Funding acquisition.

Marja Siitari-Kauppi: Resources, Supervision, Writing-Reviewing &

Editing.

References

André, M., 2009. New Methods for the Determination of Sorption Capacities and Sorption-Related Properties of Intact Rock. KTH, School of Chemical Science and Engineering (CHE), Chemical Engineering and Technology, Chemical Engineering.

André, M., Malmström, M.E., Neretnieks, I., 2009a. Determination of sorption properties of intact rock samples: new methods based on electromigration. J. Contam. Hydrol. 103, 71–81. https://doi.org/10.1016/j.jconhyd.2008.09.006.

André, M., Malmström, M.E., Neretnieks, I., 2009b. Specific surface area determinations on intact drillcores and evaluation of extrapolation methods for rock matrix surfaces. J. Contam. Hydrol. 110, 1–8. https://doi.org/10.1016/j.jconhyd.2009.05.003.

Appelo, C.A.J., 2017. Solute transport solved with the Nernst-Planck equation for concrete pores with 'free' water and a double layer. Cem. Concr. Res. 101, 102–113. https://doi.org/10.1016/j.cemconres.2017.08.030.

Appelo, C.A.J., Postma, D., 2004. Geochemistry, Groundwater and Pollution. CRC Press.

Atkins, P., Paula, J. de, 2009. Physical Chemistry, 9th edition. W. H. Freeman.

Beauwens, T., De Cannière, P., Moors, H., Wang, L., Maes, N., 2005. Studying the migration behaviour of selenate in Boom Clay by electromigration. Eng. Geol. 2003 (77), 285–293. https://doi.org/10.1016/j.enggeo.2004.07.019.

Clark, S.J., Segall, M.D., Pickard, C.J., Hasnip, P.J., Probert, M.I.J., Refson, K., Payne, M.C., 2009. First principles methods using CASTEP. Z. Kristallogr. – Cryst. Mater. 220, 567–570. https://doi.org/10.1524/zkri.220.5.567.65075.

CRC Press, 2018. CRC Handbook of Chemistry and Physics, 99th edition. .

Dai, Z., Wolfsberg, A., Lu, Z., Reimus, P., 2007. Upscaling matrix diffusion coefficients for heterogeneous fractured rocks. Geophys. Res. Lett. 34. https://doi.org/10.1029/2007GL029332.

De Cannière, P., Maes, A., Williams, S., Bruggeman, C., Beauwens, T., Maes, N., Cowper, M., 2010. Behaviour of Selenium in Boom Clay (No. SCK•C-ER-120).

de Hoog, F.R., Knight, J.H., Stokes, A.N., 1982. An improved method for numerical inversion of Laplace transforms. SIAM J. Sci. Stat. Comput. 3, 357–366. https://doi.org/10.1137/0903022.

Eklund, L., 2014. Hydration of Oxo Anions A Combined Computational and Experimental Structure and Dynamics Study in Aqueous Solutions (Doctoral thesis). Faculty of Natural Resources and Agricultural Sciences, Department of Chemistry and Biotechnology, Uppsala.

Ewing, R.C., 2015. Long-term storage of spent nuclear fuel. Nat. Mater. 14, 252–257.

García-Gutiérrez, M., Cormenzana, J.L., Missana, T., Mingarro, M., Martín, P.L., 2006. Large-scale laboratory diffusion experiments in clay rocks. In: Physics and Chemistry of the Earth, Parts A/B/C, MIGRATION 2005. 31. pp. 523–530. https://doi.org/10.1016/j.pce.2006.04.004. The 10th international conference on the chemistry and migration of actinides and fission products in the geosphere.

Grisak, G.E., Pickens, J.F., 1980. Solute transport through fractured media: 1. The effect of matrix diffusion. Water Resour. Res. 16, 719–730.

Ikonen, J., 2017. Sorption and Matrix Diffusion in Crystalline Rocks – In-Situ and Laboratory Approach (Doctoral Thesis). University of Helsinki, Finland.

Ikonen, J., Sardini, P., Jokelainen, L., Siitari-Kauppi, M., Martin, A., Eikenberg, J., 2016a. The tritiated water and iodine migration in situ in Grimsel granodiorite. Part I: determination of the diffusion profiles. J. Radioanal. Nucl. Chem. 310, 1041–1048. https://doi.org/10.1007/s10967-016-4890-6.

Ikonen, J., Voutilainen, M., Söderlund, M., Jokelainen, L., Siitari-Kauppi, M., Martin, A., 2016b. Sorption and diffusion of selenium oxyanions in granitic rock. J. Contam. Hydrol. 192, 203–211. https://doi.org/10.1016/j.jconhyd.2016.08.003.

Kuva, J., Voutilainen, M., Kekäläinen, P., Siitari-Kauppi, M., Timonen, J., Koskinen, L., 2015. Gas phase measurements of porosity, diffusion coefficient, and permeability in rock samples from Olkiluoto bedrock, Finland. Transp. Porous Media 107, 187–204. https://doi.org/10.1007/s11242-014-0432-2.

Kuva, J., Voutilainen, M., Kekäläinen, P., Siitari-Kauppi, M., Sammaljärvi, J., Timonen, J., Koskinen, L., 2016. Gas phase measurements of matrix diffusion in rock samples from Olkiluoto bedrock, Finland. Transp. Porous Media 115, 1–20. https://doi.org/10.1007/s11242-016-0748-1.

Leach, A.R., 2001. Molecular Modelling: Principles and Applications, 2nd ed. Pearson Education.

Li, X., Puhakka, E., Ikonen, J., Söderlund, M., Lindberg, A., Holgersson, S., Martin, A., Siitari-Kauppi, M., 2018. Sorption of se species on mineral surfaces, part I: batch sorption and multi-site modelling. Appl. Geochem. 95, 147–157. https://doi.org/10.1016/j.apgeochem.2018.05.024.

Löfgren, M., 2005. Diffusive Properties of Granitic Rock as Measured by In-Situ Electrical Methods. Department of Chemical Engineering and Technology, Royal Institute of Technology, Stockholm, Sweden.

Löfgren, M., 2015. Artefacts Associated with Electrical Measurements of the Rock Matrix Formation Factor. SKB SKB Report (R-14-20).

Löfgren, M., Neretnieks, I., 2006. Through-electromigration: a new method of investigating pore connectivity and obtaining formation factors. J. Contam. Hydrol. 87, 237–252. https://doi.org/10.1016/j.jconhyd.2006.05.006.

Löfgren, M., Vecernik, P., Havlova, V., 2009. Studying the Influence of Pore Water Electrical Conductivity on the Formation Factor, as Estimated Based on Electrical Methods. SKB Report R-09-57.

Maes, N., Moors, H., Dierckx, A., De Cannière, P., Put, M., 1999. The assessment of electromigration as a new technique to study diffusion of radionuclides in clayey soils. J. Contam. Hydrol. 36, 231–247. https://doi.org/10.1016/S0169-7722(98)00146-6.

Mattsson, K.-J., Rauséus, G., Eklund, S., 2007. Oskarshamn Site Investigation. Boremap Mapping of Core Drilled DFN Boreholes KLX11B–KLX11F. SKB report, P-06-244.

Melnyk, T.W., Skeet, A.M.M., 1986. An improved technique for the determination of rock porosity. Can. J. Earth Sci. 23, 1068–1074. https://doi.org/10.1139/e86-107.

Meng, S., Li, X., Siitari-Kauppi, M., Liu, L., 2019. Development and application of an advection-dispersion model for data analysis of electromigration experiments with intact rock cores. J. Contam. Hydrol Submitted for publication.

Mitchell, J.K., Soga, K., 2005. Fundamentals of Soil Behavior. John Wiley & Sons.

Möri, A., Mazurek, M., Adler, M., Schild, M., Siegesmund, S., Vollbrecht, A., Ota, K., Ando, T., Alexander, W.R., Smith, P.A., Haag, P., Bühler, C., 2003. The Nagra-JNC In Situ Study of Safety Relevant Radionuclide Retardation in Fractured Crystalline Rock IV: The In Situ Study of Matrix Porosity in the Vicinity of a Water Conducting Fracture. Nagra Technical Report 00–08.

Muuri, E., 2015. The Sorption and Diffusion of Ba-133 in Granitic Rocks (Master thesis). University of Helsinki, Finland.

Neretnieks, I., 1980. Diffusion in the rock matrix: an important factor in radionuclide retardation? J. Geophys. Res. Solid Earth 85, 4379–4397. https://doi.org/10.1029/JB085iB08p04379.

NIST Chemistry WebBook, SRD 69, 2018. Quinoxaline. [WWW Document]. URL. https://webbook.nist.gov/cgi/cbook.cgi?ID=C91190&Mask=400#UV-Vis-Spec.

Norton, D., Knapp, R., 1977. Transport phenomena in hydrothermal systems: the nature of porosity. Am. J. Sci.; (United States) 277. https://doi.org/10.2475/ajs.277.8.913.

Ohlsson, Y., 2000. Studies of Ionic Diffusion in Crystalline Rock. Department of Chemical Engineering and Technology, Royal Institute of Technology, Stockholm, Sweden.

Ohlsson, Y., Neretniks, I., 1997. Diffusion Data in Granite. Recommended values (No. SKB Reprot TR-97-20). Swedish Nuclear Fuel and Waste Management Co.

Posiva, Oy, 2012. Safety Case for the Disposal of Spent Nuclear Fuel at Olkiluoto-Features, Events and Processes 2012. Posiva Reoprt 2012-07.

Posiva, Oy, 2013. Safety Case for the Disposal of Spent Nuclear Fuel at Olkiluoto. Models and Data for the Repository System 2012. Parts 1 and 2. Posiva Oy, POSIVA Report 2013-1.

Puukko, E., 2014. Sorption of Cesium in Intact Rock. Posiva Oy, Posiva Report 2014-13.

Puukko, E., Lehto, J., Lindberg, A., Voutilainen, M., 2018. Electromigration experiments for studying transport parameters and sorption of cesium and strontium on intact crystalline rock. J. Contam. Hydrol. 217, 1–7. https://doi.org/10.1016/j.jconhyd.2018.08.010.

Séby, F., Potin-Gautier, M., Giffaut, E., Donard, O.F.X., 1998. Assessing the speciation and the biogeochemical processes affecting the mobility of selenium from a geological repository of radioactive wastesto the biosphere. Analusis 26, 193–198. https://doi.org/10.1051/analusis:1998134.

Skagius, K., 1986. Diffusion of Dissolved Species in the Matrix of some Swedish Crystalline Rocks. Royal Institute of Technology, Stockholm, Sweden.

Skagius, K., Neretnieks, I., 1983. Diffusion Measurements in Crystalline Rocks. Royal Institute of Technology, Stockholm, Sweden.

Söderlund, M.J., 2016. Sorption and Speciation of Radionuclides in Boreal Forest Soil (Doctoral thesis). University of Helsinki, Finland.

Söderlund, M., Hakanen, M., Lehto, J., 2016a. Sorption of cesium on boreal forest soil I: the effect of grain size, organic matter and mineralogy. J. Radioanal. Nucl. Chem. 309, 637–645. https://doi.org/10.1007/s10967-015-4612-5.

Söderlund, M., Virkanen, J., Holgersson, S., Lehto, J., 2016b. Sorption and speciation of selenium in boreal forest soil. J. Environ. Radioact. 164, 220–231. https://doi.org/10.1016/j.jenvrad.2016.08.006.

Tachi, Y., Ebina, T., Takeda, C., Saito, T., Takahashi, H., Ohuchi, Y., Martin, A.J., 2015. Matrix diffusion and sorption of Cs+, Na+, I– and HTO in granodiorite: laboratory-scale results and their extrapolation to the in situ condition. J. Contam. Hydrol. 179, 10–24. https://doi.org/10.1016/j.jconhyd.2015.05.003.

Yu, J.-W., Neretnieks, I., 1997. Diffusion and Sorption Properties of Radionuclides in Compacted Bentonite (No. SKB-TR–97-12). Swedish Nuclear Fuel and Waste Management Co.